

# MEASURING INSTRUMENTS FOR HYPERABRUPT VARACTOR TUNING DIODES

By

A. AMBRÓZY, P. GOTTWALD and V. SZÉKELY

Department of Electron Tubes and Semiconductors. Technical University.  
Budapest

(Received February 21. 1970)

Presented by Prof. Dr. I. P. VALKÓ

## Introduction

The capacitance of a reverse biased pn junction was observed for the first time by SCHOTTKY in 1929 who published a good approximating theory in 1942 [1]. The modern transistor technology rendered possible to make pn junctions with reproducible capacitance *vs* reverse bias  $[C(U_R)]$  curves. Fig. 1 compares some typical impurity profiles and the obtainable  $C(U_R)$  curves.

It may be seen that the "classical" technologies realize  $n = -1/2$  even in the best case. These devices have been suitable for some purposes, e.g. AFC, FM, parametric amplifying, frequency multiplying etc. In broadcasting or in professional communication, however, the usual relative bandwidth is 1 : 2 ... 1 : 3, so the problem of making pn junctions with 1 : 5 ... 1 : 10 capacitance ratio has been raised. Generally matched diode pairs, triplets or quadruplets are needed.

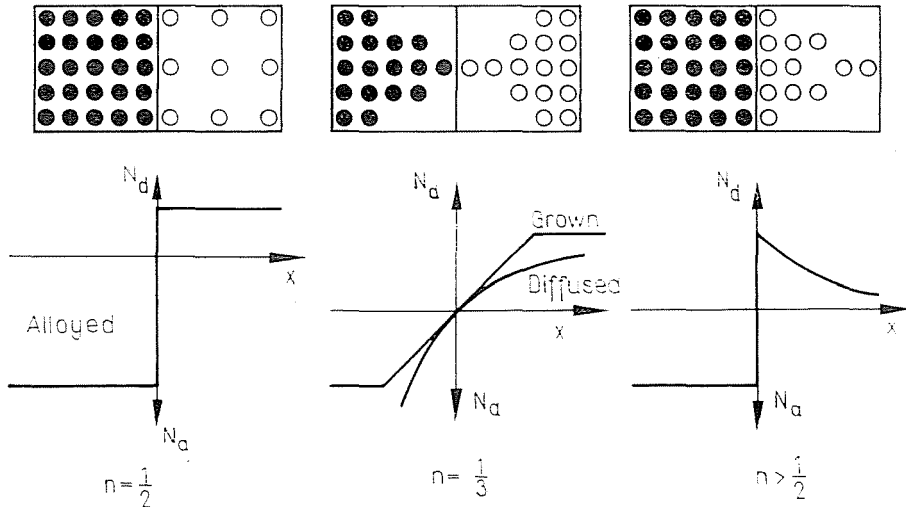


Fig. 1. Various impurity profiles

Fig. 1c shows the required hyperabrupt impurity profile which may be realized combining diffusion and alloying or by programmed epitaxial growth. It may be shown [2] that if the one side (in our case the  $p$ ) is heavily doped and in the other the net impurity density depends on  $x$  (the distance from the junction) as

$$N = N_d - N_a = Bx^m, \quad (1)$$

then

$$C = \frac{dQ}{dU_R} = A \left[ \frac{qB\varepsilon^{m+1}}{(m+2)(U_R + U_D)} \right]^{\frac{1}{m-2}}, \quad (2)$$

where  $A$  is the junction area,  $\varepsilon = \varepsilon_0\varepsilon_r$  the absolute permittivity of the semiconductor material,  $U_R$  and  $U_D$  are the reverse bias and built-in voltages, respectively.

If Eq. (2) is rewritten as

$$C = k(U_R + U_D)^{-n} \quad (3)$$

it is evident that  $n = 1/(m+2)$  and  $n > 0.5$  requires  $m < 0$ .

The junction capacitance is inherently associated with a series resistance. Supposing one dimensional structure and neglecting the resistance of the  $p$ -side

$$r_s = \int_w^l \frac{\rho}{A} dx = \int_w^l \frac{dx}{Aq\mu_n Bx^m} = \frac{1}{Aq\mu_n B} \frac{1}{1-m} (l^{1-m} - w^{1-m}), \quad (4)$$

where  $l$  is the total length of the  $n$ -side,  $w$  is the depletion layer width,  $\mu_n$  the electron mobility (considered roughly constant). Higher capacitance ratio needs greater  $|m|$  and/or  $l$ . Since  $1-m > 1$  in all hyperabrupt structures, the improvement of capacitance ratio, breakdown voltage and  $r_s$  are in contradiction [3].

Both the manufacturer and the user of the diodes wish to know the following characteristics:

- 1)  $C$  vs  $U_R$  in the full range of operation
- 2)  $C(U_{R1})/C(U_{R2})$  at preselected  $U_{R1}$  and  $U_{R2}$
- 3)  $dC/dU$  at a given  $C_0$  or  $U_R$
- 4) Matching of  $C(U_R)$  curves of diode triplets or quadruples
- 5) Series resistance

Our project was to find the suitable measuring principles and to build prototype instruments.

**Measurement of diode capacitance and capacitance ratio**

Although the required accuracy of capacitance measurement would have demanded a bridge circuit, it was dropped for the sake of rapid, direct reading and compatibility to capacitance ratio measuring circuit. Fig. 2 shows that the diode to be measured is connected to a voltage generator and

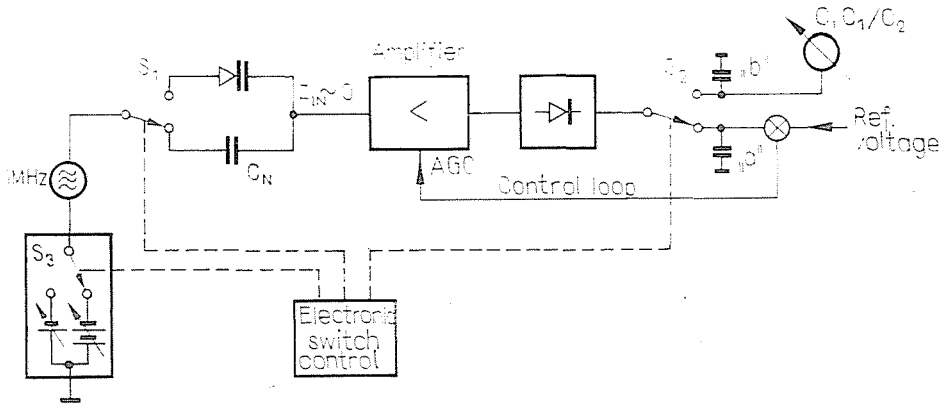


Fig. 2. Block diagram of the capacitance and capacitance ratio measuring instrument

to a low input impedance current amplifier. If  $|1/j \omega C| \gg Z_{in}$ , the input current is directly proportional to  $C$ . The low impedance levels effectively reduce the sensitivity with regard the outer disturbances.

As it can be seen in Fig. 2 the electronic switch S1 connects either the diode or a precisely known capacitor  $C_n$  into the measuring circuit. Fig. 3 shows the amplified and detected waveform. A second switch S2 samples this signal and the samples are stored in two capacitors. Stored sample "a" is kept constant by a control loop consists of a comparator and the variable

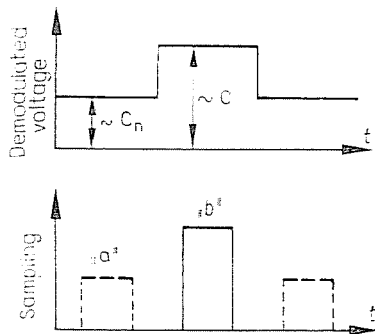


Fig. 3. Demodulator output and sampling waveform

gain HF amplifier. Then sample "b" is proportional to the diode capacitance  $C$ . The accuracy depends on the sampling accuracy and on the control loop gain.

The loop gain is not constant because of the nonlinear gain characteristic of the amplifier; however, an 1 : 3 change in the reference input causes only 3 per cent deviation of the output signal "a". Actually, the reference input does not change more than one per cent since the generator amplitude is stabilized.

In the three measuring ranges (1—3.16—10—31.6 pF) only one normal capacitor is used, connected to three different taps of a precision transformer.

The principle and circuit treated above may easily be extended to measure capacitance ratio. Now S1 (Fig. 2) permanently connects the diode to be measured into the circuit and disconnects  $C_n$ . Then the lower diode capacitance, measured at higher reverse bias, serves as reference input. S3 switches the higher (0...30 V) and the lower (0...10 V) bias. Referred to Fig. 3, now sample "a" — which is kept always constant — corresponds to the capacitance ratio.

### Measurement of the $dC/dU$ slope

Besides the capacitance ratio another — near equivalent — figure of merit of the diode is the  $dC/dU$  slope. Fig. 4 shows the block diagram of a  $dC/dU$  meter. The diode to be measured is reverse biased by the voltage

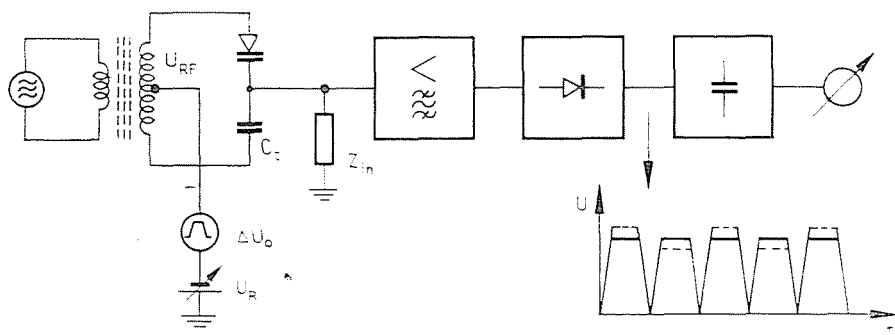


Fig. 4. Block diagram of  $dC/dU$  measurement

source  $U_R$  through the transformer windings and the amplifier input resistance. The superimposed low frequency trapezoidal voltage  $\Delta U_0$  modulates the reverse bias ( $\Delta U_0 \ll U_R$ ), hence the capacitance of the diode changes by  $\Delta C$ . A symmetrical RF bridge is formed from the differential transformer, diode and variable capacitor  $C_0$ . The RF voltage  $U_{RF}$  on the diode is much lower than  $\Delta U_0$ , usually a few tens of millivolts.

For a crude first approximation let us suppose that there are linear relationships between bridge output voltage and  $\Delta C/C_0$  as well as  $C$  and  $U_R$ .

According to Fig. 4 the amplified and envelope detected bridge output voltage consists of a train of trapezoids with equal heights assuming balanced bridge and above approximations. Out of balance results in higher and lower trapezoids by pairs. A peak voltmeter indicates always the higher one.

Measurement of  $dC/dU$  at a prescribed  $C_0$  is very simple: Set the deflection of the peak voltmeter to a minimum by adjusting  $U_R$  and read this deflection which is proportional to  $(dC/dU) \Delta U_0$ . A more detailed analysis, considering nonlinearities and losses, as well as applications are published elsewhere [4].

### Semiautomatic sorter

The main user of hyperabrupt tuning diodes today is the TV-receiver industry. The front-end tuners need 3 or 4 matched diodes. The matching conditions are severe: only a few (usually 3) per cent deviation is allowed

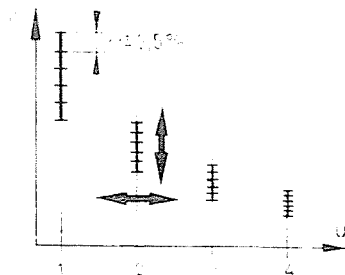


Fig. 5. Capacitance classes at matching points

among the capacitances over the whole range of operation. Rigorously, this may be checked only on preselected diodes and the resulting deviation curves represent theoretically an infinite number of measured points.

For sorting purposes the number of matching points (where the deviation is definitely limited) must be as low as possible. Since the diodes — according to their deviation from a reference capacitance — may fall into different classes at any matching point, an  $n$ -dimensional matrix is needed to characterize (and in fact, to store) the diodes, where  $n$  is the number of matching points.

Preliminary analysis showed and factory experiences verified that lower performance diodes demand two-point matching while higher performance ones three or four points. Five or six classes were sufficient in each case. The class width was reduced to 2.5 per cent (Fig. 5).

To avoid the huge number of matrix cells (600—900) two-step sorting is used for high performance diodes. During the pre-sorting, classification in

two working points assigns the place of the diode in a  $6 \times 5 = 30$  cell "large" matrix (see Fig. 6). The necessary number of pieces to be pre-sorted is in order of 10 000. Many hundred pieces assemble in each cell.

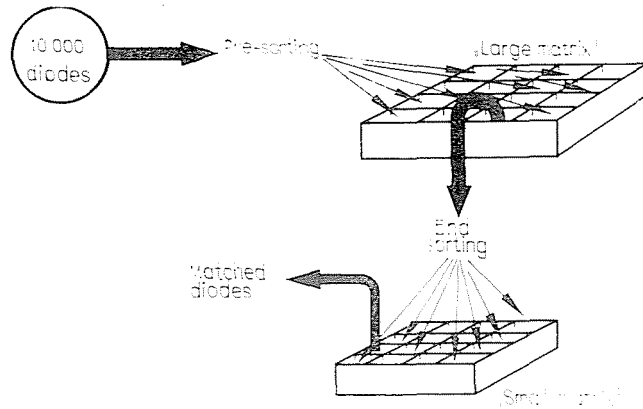


Fig. 6. Sorting process

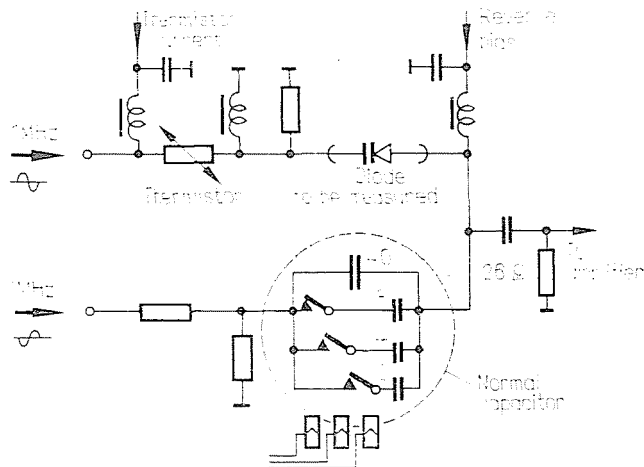


Fig. 7. Bridge circuit for sorting

The end-sorting takes place in two other working points. The content of one cell of the large matrix is sorted to the  $6 \times 5$  cell "small" matrix. Since the full sorting process demands a long time, good long-term stability is necessary.

The measuring circuit is shown in Fig. 7. With opposite phase feeding, the two arms form a bridge which in general is not totally balanced. The classification of the diode to be measured takes place by stepwise change of

normal capacitor until approximating the best balance. The 2—4—8 pF part-capacitors give 5 per cent ( $2 \times 2.5$ ) increments approximately, in a binary order.

Rapid switching from one working point to another demands rapid change bridge arm ratio. This is achieved by a direct heated thermistor divider. The heating current is provided by a DC control circuit which compares the thermistor resistance with a precision, variable resistance. By means of the latter the nominal value of the capacitance to be measured may be set (see Fig. 5, vertical arrow).

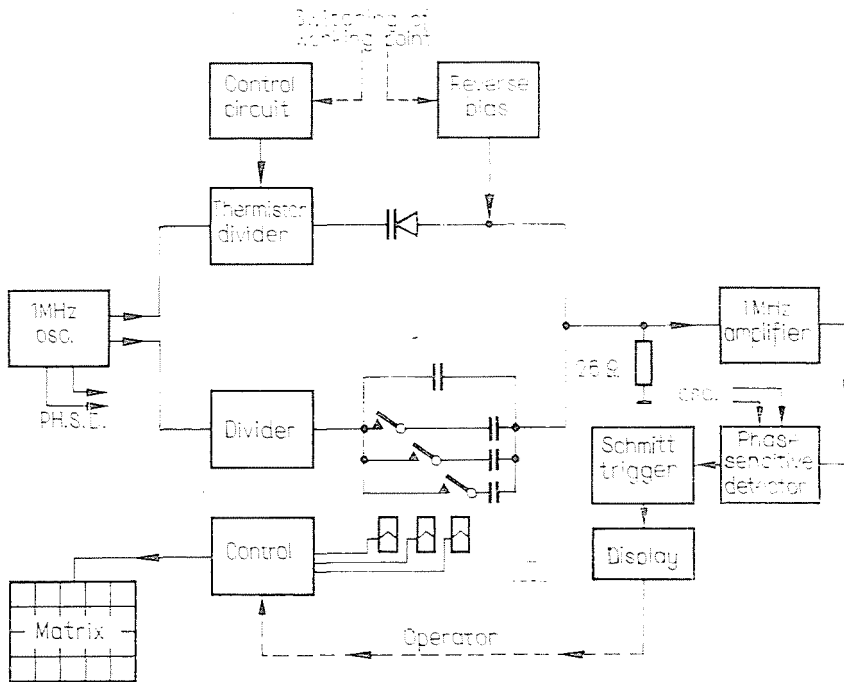


Fig. 8. Block diagram of the diode sorter

Fig. 8 shows the block diagram of the diode sorter. The amplified bridge output voltage is phase sensitive detected and controls two Schmitt-trigger which are connected to one green and two yellow display lamps. At the best bridge balance the green lamp lights. To obtain this condition the operator should change the normal capacitor by turning a rotary switch in the appropriate direction showed by one of the yellow lamps. Repeating this process in an other matching point (by another rotary switch, since the former stores an information about the first point) one cell of the pre-sorting matrix may be assigned by lighting a small bulb. The end-sorting is similar.

The realized prototype of the diode sorter operates as described above.

In an advanced version the rotating switches and sequence control may easily be replaced by digital circuits without abandoning the principle described.

### Measurement of the series resistance

The diode to be measured serves as a capacitive load of a coaxial resonator (Fig. 9). The one lead of the diode is fixed inside of the center conductor by a slotted springing cone, the other by three bored metal sheets slipping on one another.

According to the equivalent circuit of Fig. 10, the resonator is fed by a constant frequency generator whose transformed equivalent EMF and inner resistance are  $u$  and  $r_g$ , respectively. The circuit may be tuned to resonance by proper biasing of the diode. The width of the resonance curve depends on  $r_s$ . Using modulated bias this curve can be swept between two points having equal heights, say  $1/\sqrt{2}$  fraction of the peak value. In this case

$$r_s = \frac{1}{2\pi C_0} \frac{\Delta C}{C_0} = \frac{1}{2\pi C_0^2} \frac{dC}{dU} \Big|_{C_0} \Delta U. \quad (5)$$

Since  $C_0$  is fixed and  $dC/dU$  may be measured (see above)  $\Delta U$  is characteristic of  $r_s$  unambiguously.

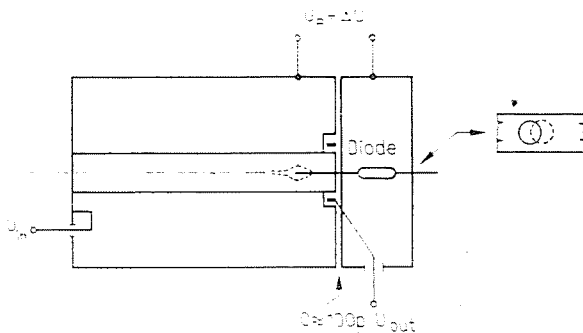


Fig. 9. Outlines of the coaxial resonator

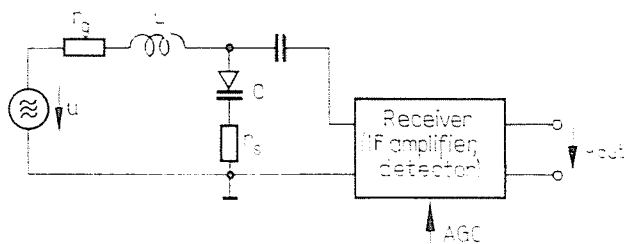


Fig. 10. Equivalent circuit of the resonator



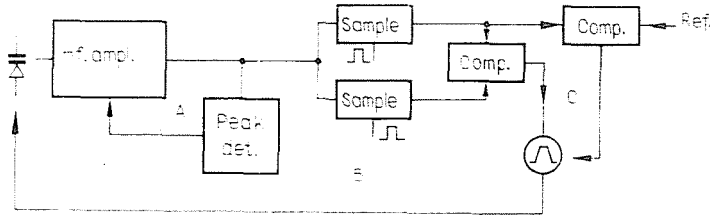


Fig. 11. Block diagram of the control loops

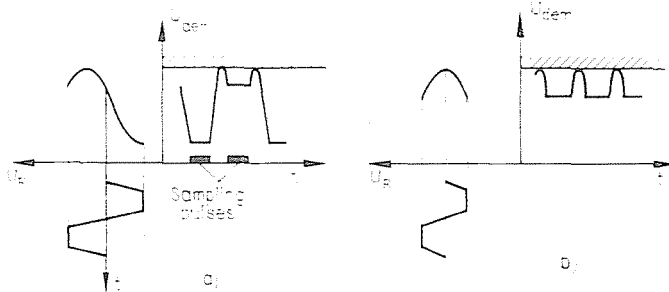


Fig. 12. Demodulated waveforms: a) initial condition, b) stationary condition

Unwanted components (e. g. generator series resistance, stray capacitance of the diode holder) complicate this simple expression. Generally

$$r_s = X(r_s) \frac{dC}{dU} \Big|_{C_0} \Delta U, \tag{6}$$

where

$$X(r_s) = \frac{\text{const}}{\left[ 1 + \frac{r_g}{r_s} \left( 1 + \frac{\Delta C}{C_0} \right) \right]} \tag{7}$$

which is a slowly varying function of  $r_s$ , keeping  $r_g$  as low as possible.

The realized circuit contains three feedback loops (Fig. 11). Loop A fixes the peak of the resonance curve, i.e. the peak value of the amplified and detected signal, by controlling the AGC. During this, the diode reverse bias has a large amplitude modulation and the detected waveform is generally asymmetrical (Fig. 12a). Then the loop B samples the "valleys" and tends to qualize them. Finally, loop C reduces the modulating trapezoid amplitude until the valleys are equal to the reference voltage (about 70 per cent of the peak). According to Eq. (6),  $\Delta U$  is directly proportional to  $r_s$ . The scale factor may be set by a previous  $dC/dU$  measurement which is very quick using the circuit of Fig. 4. Sorted diodes, belonging to the same group, require only one  $dC/dU$  setting.

### Summary

Electronic tuning of resonant circuits in the RF, VHF and UHF ranges has lead to the development of hyperabrupt tuning varactor diodes. These nonlinear and lossy devices raised new measuring problems. Five of them, namely: capacitance, capacitance ratio, matching of  $C(U)$  curves,  $dC/dU$  slope and series resistance are treated and the principal design of the measuring instruments are outlined.

### References

1. SCHOTTKY, W.: Vereinfachte und erweiterte Theorie der randschicht Gleichrichter. *Z. Phys.* **118**, 539–592 (1942).
2. NORWOOD, M. H. — SHATZ, E.: Voltage variable capacitor tuning: a review. *Proc. IEEE* **56**, 788–798 (1968).
3. LEE, T. P.: Calculations of cutoff frequency, breakdown voltage, and capacitance for diffused junctions in thin epitaxial silicon layers. *IEEE Trans. on El. Dev.* **ED-13**, 881–896 (1966).
4. AMBRÓZY, A.: A simple  $dC/dV$  measurement method and its applications. *Solid State El.* **13**, 347–353 (1970).
5. II. Országos Elektronikus Műszer- és Mérőtechnikai Konferencia kiadványa, 269–304. Budapest, 1969. június.

Dr. András AMBRÓZY  
Péter GOTTWALD  
Vladimir SZÉKELY

} Budapest XI., Műegyetem rkp. 9. Hungary